International Journal of Mechanical, Industrial and Aerospace Sciences
ISSN: 2517-9950
Vol:6, No:11, 2012

CFD Modeling of a Radiator Axial Fan for Air Flow Distribution

S. Jain, and Y. Deshpande

***Abstract*—**The fluid mechanics principle is used extensively in designing axial flow fans and their associated equipment. This paper presents a computational fluid dynamics (CFD) modeling of air flow distribution from a radiator axial flow fan used in an acid pump truck Tier4 (APT T4) Repower. This axial flow fan augments the transfer of heat from the engine mounted on the APT T4.

CFD analysis was performed for an area weighted average static pressure difference at the inlet and outlet of the fan. Pressure contours, velocity vectors, and path lines were plotted for detailing the flow characteristics for different orientations of the fan blade. The results were then compared and verified against known theoretical observations and actual experimental data. This study shows that a CFD simulation can be very useful for predicting and understanding the flow distribution from a radiator fan for further research work.

***Keywords*—**Computational fluid dynamics (CFD), acid pump truck (APT) Tier4 Repower, axial flow fan, area weighted average static pressure difference, and contour plots.

I. Introduction and Background

THE axial flow fan is extensively used in many engineering applications. Its adaptability has resulted in implementation into large scale systems, from industrial dryers and air conditioning units to automotive engine cooling and in-cabin air recirculation systems. The benefit of using axial flow fans for the purpose of augmenting heat transfer is particularly evident in the automobile industry because of the need for relatively compact designs. The extended use of axial flow fans for fluid movement and heat transfer has resulted in detailed research into the performance attributes of many designs [1], [2]. Numerical investigations have been performed to quantify the performance of axial fans and their flow characteristics [3], [4]. However, the more-practical example of cooling a heated engine or heated plate using an axial flow fan has received more attention in regards to understanding flow characteristics and heat transfer [5]-[7]. Moreover, an additional practice for monitoring axial fan performance is by using the experimental technique discussed in this paper.

With the expressive computer capability and extensive development in the simulation field, CFD have drawn attention in recent years. With the help of CFD, the complex 3-D geometries of equipment can now be modeled with only minor simplifications. CFD models, if created correctly, can account for the complex flows in equipment. CFD models for axial fans have been used to evaluate the flow behavior and characteristics. The models provide sufficiently accurate predictions over a range of operating conditions, which are not possible using other methods. Without an understanding of the characteristics of air flow passing through a fan, problems related to engine cooling systems can never be fully resolved. In this paper, CFD were used to model the flow passing through a radiator fan, which was then compared with actual experimental data.

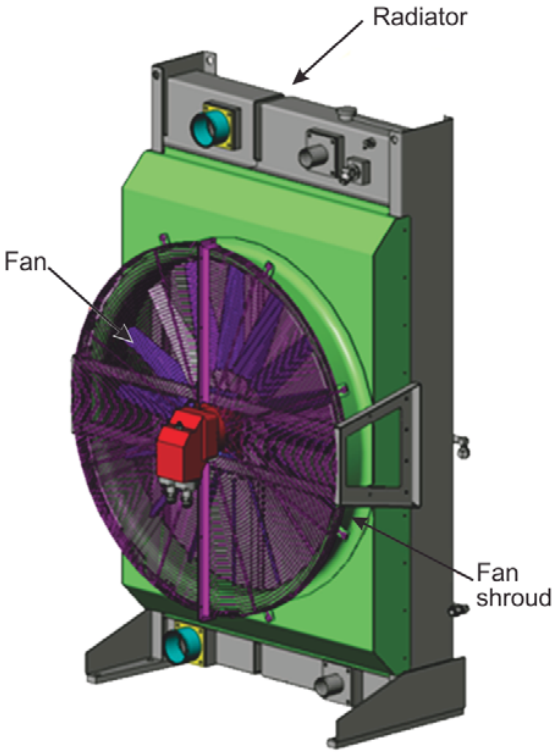

Fig. 1 Radiator and fan assembly

An APT T4 repower radiator fan and fan shroud (Fig. 1) play a crucial role in complicated engine cooling systems, such as the one shown in Fig. 2. A radiator (Figs. 1 and 2) is a type of heat exchanger designed to transfer thermal energy from the coolant to the surrounding air by means of a mechanism known as natural or forced convection. The latter case concerns the use of a radiator fan to pull the air through the radiator core.

F. S. Jain is with Halliburton Technology Center, Pune 411001 India (phone: +91-20-40158000; fax: +91-20-40158199; e-mail: Siddharth.Jain@halliburton.com).

S. Y. Deshpande is with Halliburton Technology Center, Pune 411001 India, (e-mail: Yogesh.Deshpande@halliburton.com).

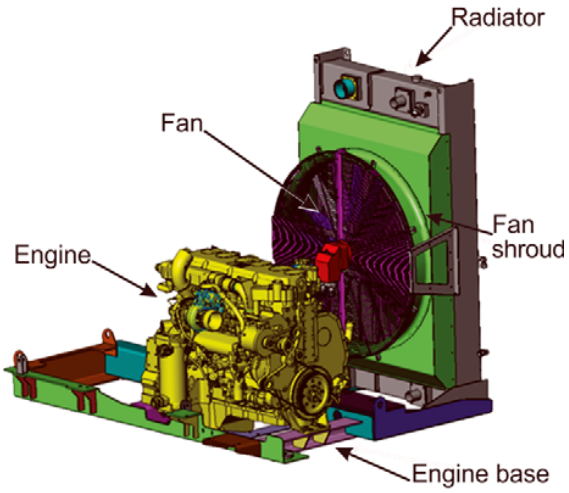

Fig. 2 Cooling system

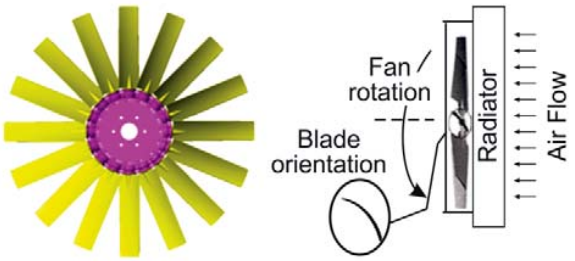

Fig. 3 Right oriented blade

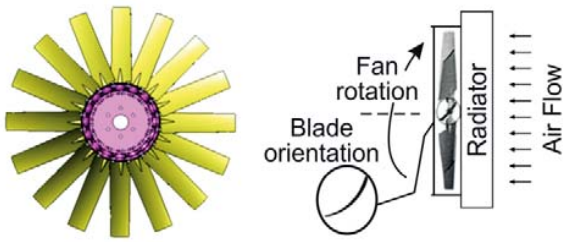

Fig. 4 Left oriented blade

The fan provides air flow through the radiator. The orientation of the blade also plays an important role in understanding the flow of air across the radiator and fan. Figs. 3 and 4 show a fan and its associated orientation configuration. For a right oriented blade, the direction of fan rotation is clockwise; for a left oriented blade, the direction of fan rotation is counterclockwise.

II. Numerical CFD Model and Procedure

The first step is to identify a typical radiator axial flow fan that can be reproduced as a 3-D CAD Solidworks® software engineering drawing package (Fig. 5).

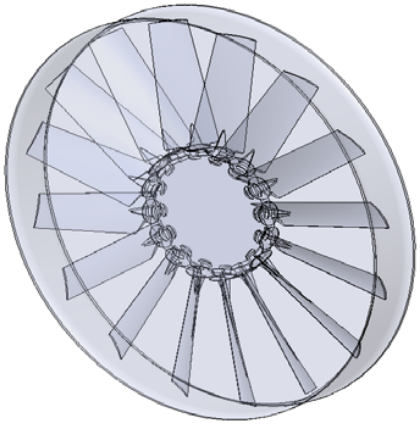

Fig. 5 Computational domain of a fan

The 3-D models are then imported into the CFD software, remodeled into different sections, and refined to generate a finite volume meshing (Fig. 6). This is a crucial step, where details of the geometrical shape need to be defined precisely. The flow domain is also created, and the final meshing of all components needs to be accurate. The total element count will be around 1.6 million, with an inflation layer on the blades. Any errors in the drawings and flow area need to be corrected before continuing.

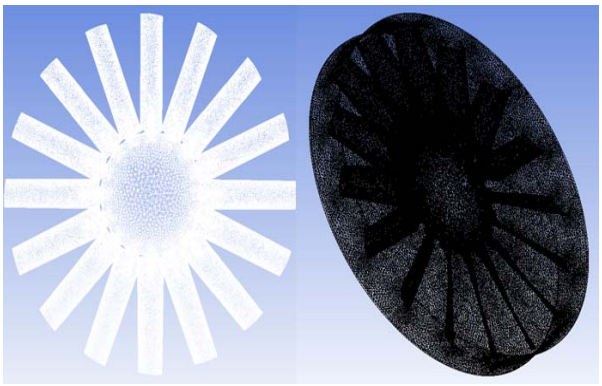

Fig. 6 Meshing of Rotor and Computational Domain

The second step is to import the files into the CFD code preprocessor, which will solve the flow equations. Here, the flow fields boundary conditions are set. These include inlet air mass flow, outlet pressure, fluid properties, and flow domain characterization, such as moving internal zone and stationary solid walls. The next step is to set the simulation process as a 3-D steady and turbulent problem (Fig. 7).

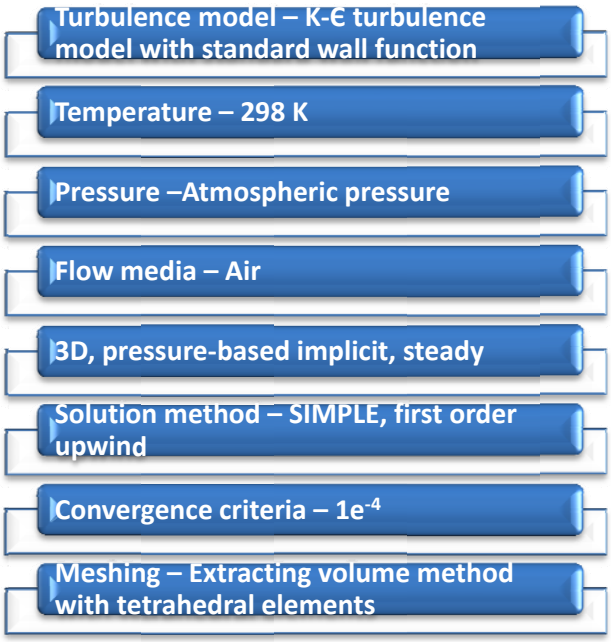

Fig. 7 Simulation parameters

The simulation is preceded with the CFD code processing the data, applying the basic theory of fluid mechanics by balancing the mass continuity and momentum equations in numerical form and thereafter producing numerical predictions of the flow variables. The problem setup process is completed by defining the boundary conditions, solver controls, and convergence monitors. Assuming the flow to be ideal and dry air at standard atmospheric pressure, the boundary conditions include fixed wall, moving internal zone at 1,680 rev/min, zero pressure at outlet, and variable mass flow rate at inlet. The residual values of all variables solved are monitored during the iteration process, with mass balance set to less than $1.0E^{-4}$. This iteration process needs to be monitored for convergence and repeated if the numerical error conditions are not satisfied. The final step is to analyze the output data and present them in the form of velocity vector distribution and contour plots.

III. Results and Discussion

On post-processing the numerical CFD results, the observations are presented as velocity vector distributions, flow lines, and static pressure contour plots at the inlet and outlet. Experimental results are then compared with CFD results for pressure difference and presented in the form of graphs. For the velocity vector representation, a plane is taken normal to the x-axis coordinate and at the center (0, 0, 0). Results are compiled separately for left and right oriented blades.

A. Left Oriented Blade

For a left oriented blade, results were compiled for air flowing at a mass flow rate of 25.26 kg/s and fan rotation of 1,680 rev/min in a counterclockwise direction and having the outlet pressure as atmospheric. Fig. 8 shows the velocity magnitude on the rotor for a left oriented blade. It states that velocity increased moving from the hub to the tip on the rotor and thus confirmed the theoretical concept of $V = r.\omega$. This certainly verifies that the rotor rotated exactly at the center of the fan axis.

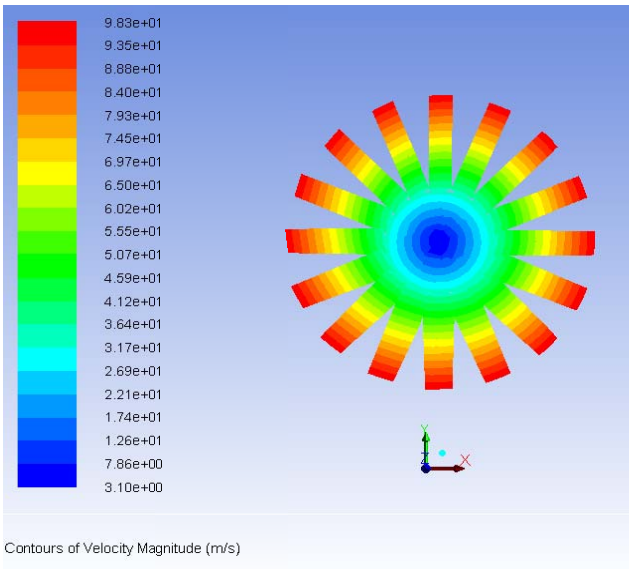

Fig. 8 Velocity magnitude on rotor

Figs. 9a and 9b show the pressure contours for static pressure at the inlet and outlet of the axial fan for a left oriented blade. By observing the pressure contour at the inlet, pressure ranges on negative scale, and at the outlet, pressure ranges from negative to positive scale; hence, creating a positive pressure zone at the outlet side, which coincided with the theoretical characteristics of fan performance.

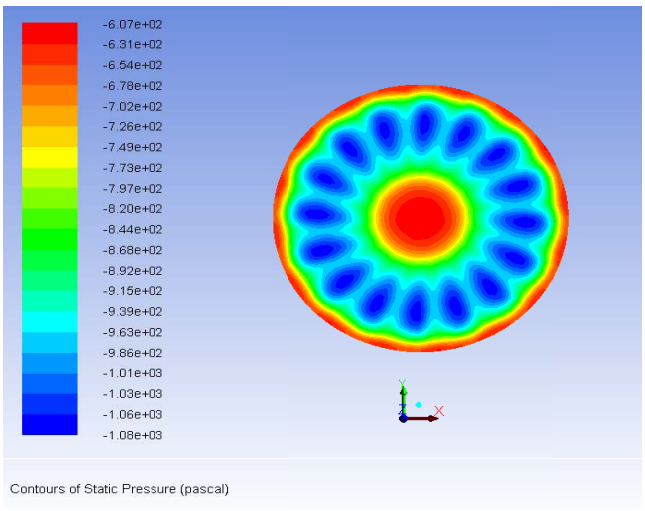

Fig. 9a Static pressure at inlet

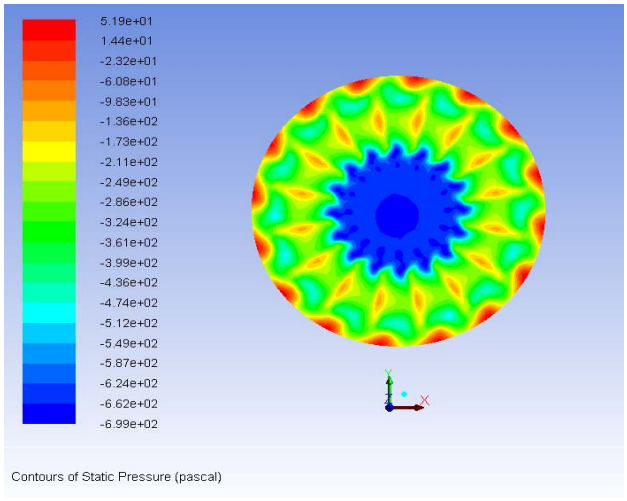

Fig. 9b Static pressure at outlet

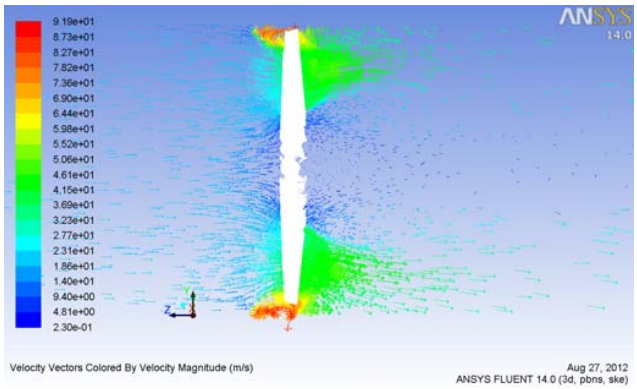

Fig. 10a Velocity vector distribution

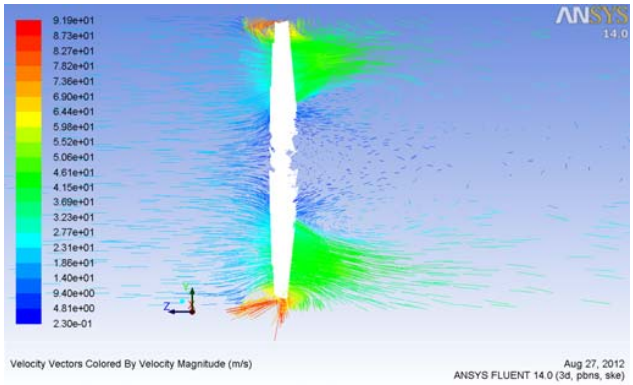

Fig. 10b Flow lines around rotor

Figs. 10a and 10b show the velocity vector distribution and flow lines at a plane normal to the x-axis and perpendicular to the rotor. A high flow region formed around the outer diameter of the flow domain and a low reverse flow region formed in the center behind the fan hub. Between the high and low reverse flow regions, there existed strong circulation vortices. Strong circulation regions were also observed behind the fan blades. This helps in understanding the flow behavior around the rotor with a left oriented blade.

Experimental measurements were performed on a Tier4 unit for the radiator axial flow fan. The experiments were performed at atmospheric pressure having standard SAE condition at 77°F and 300 ft. Several different points were considered on the fan inlet and outlet face for measuring static pressure and air flow. With the help of transducers and a data acquisition system, static pressure and air flow (cubic feet per minute) were measured at different points, which were spaced over the inlet and outlet face of the fan. Later, air flow in CFM was converted into mass flow rate (kg/s). Average values of these points were considered to compare with CFD results.

Fig. 11 shows a comparison of axial fan experimental and numerical CFD performance with a left oriented blade. The static pressure (in terms of H_20) was plotted for a variable mass flow rate of 10, 14.6, 25.26, 32.26, 36.7, 39.544, and 41.97 kg/s. The graph demonstrates the same trend curve and values for both the experimental and numerical CFD results. The insignificant disparity in the results could be a result of experimental conditions, fluctuations of fan rev/min, or the considered ideal condition while simulating the analysis.

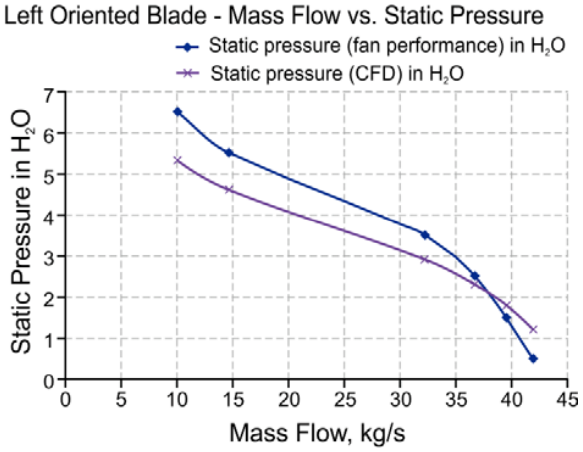

Fig. 11 Experimental vs. CFD performance

B. Right Oriented Blade

For a right oriented blade, results were compiled for the same working conditions as for the left oriented blade—air flowing at a mass flow rate of 25.26 kg/s and fan rotation of 1,680 rev/min in a clockwise direction and having the outlet pressure as atmospheric. Fig. 12 illustrates the velocity magnitude on the rotor with a right oriented blade, which confirms that velocity increased moving from the hub to the tip on the rotor and thus validated the theoretical concept of $V= r.\omega$. This also affirms that the rotor was rotating at the center point of the fan axis.

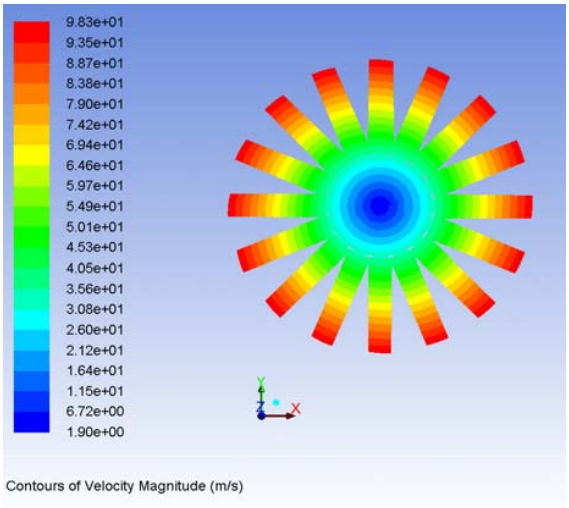

Fig. 12 Velocity magnitude on rotor

Figs. 13a and 13b show the pressure contours for static pressure at the inlet and outlet of the axial fan with a right oriented blade. By observing the pressure contour at the inlet, pressure varies on negative scale, and at the outlet, pressure varies from negative to positive scale; thus, creating a pressure zone at the outlet. This is in accordance with the theoretical observation, and the pressure zone conditions were similar to that of fan with a left oriented blade.

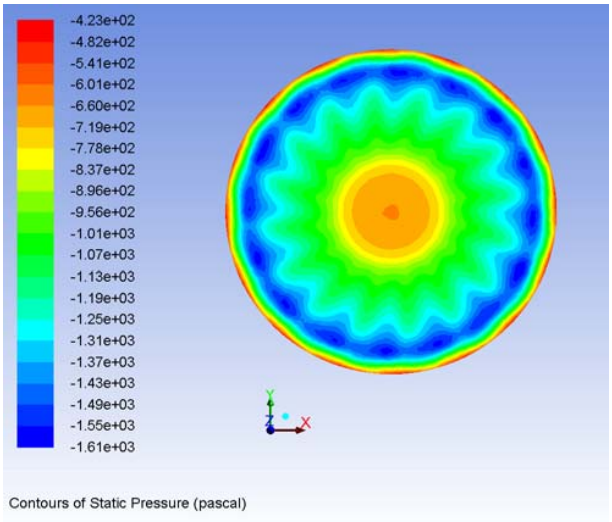

Fig. 13a Static pressure at inlet

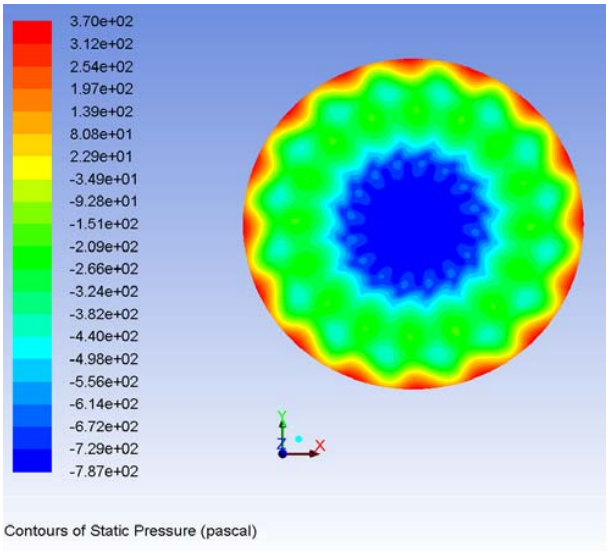

Fig. 13b Static pressure at outlet

Figs.14a and 14b show the velocity vector distribution and flow lines at a plane normal to the x-axis and perpendicular to the rotor. Again, a high flow region formed around the outer diameter of the flow domain (i.e., at the tip side of the blade). Also, a low reverse flow region formed in the center behind the fan hub. There existed strong circulation vortices in between the high and low reverse flow regions. Similar strong circulation regions were also observed behind the fan blades as those seen in a fan with a left oriented blade. This is useful in understanding the flow behavior around the rotor with a right oriented blade.

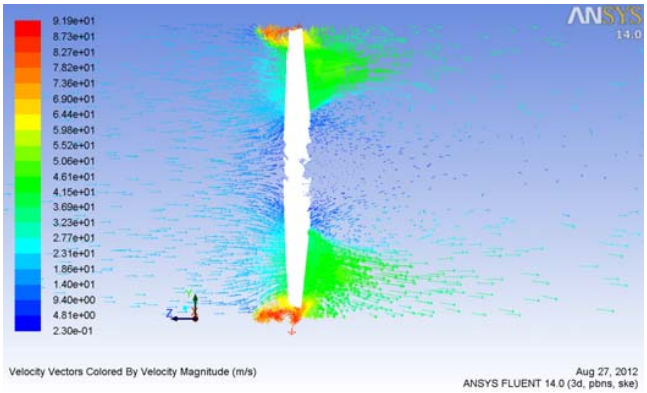

Fig. 14a Velocity vector distribution

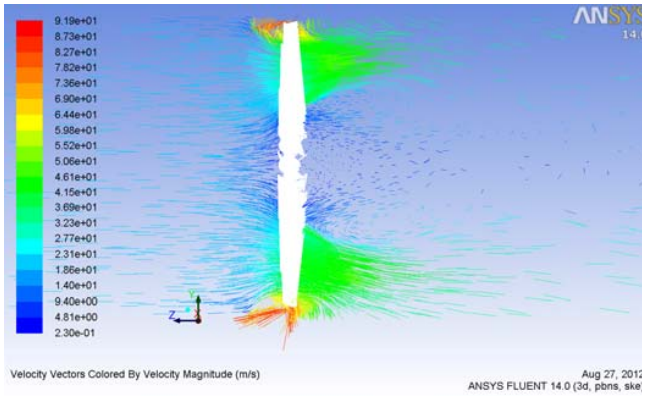

Fig. 14b Flow lines around rotor

A similar experimental setup was been used for a right oriented blade as was used for the left oriented blade.

Fig. 15 shows a comparison of the experimental and numerical CFD performance of the axial fan. The static pressure (in terms of H_20) was plotted for a variable mass flow rate of 10, 14.6, 25.26, 32.26, 36.7, 39.544, and 41.97 kg/s. The graph demonstrates the same trend curve and values for both the experimental and numerical CFD results. The nominal difference in the results could be a result of experimental conditions, fluctuations of fan rev/min, or the considered ideal condition while simulating the analysis.

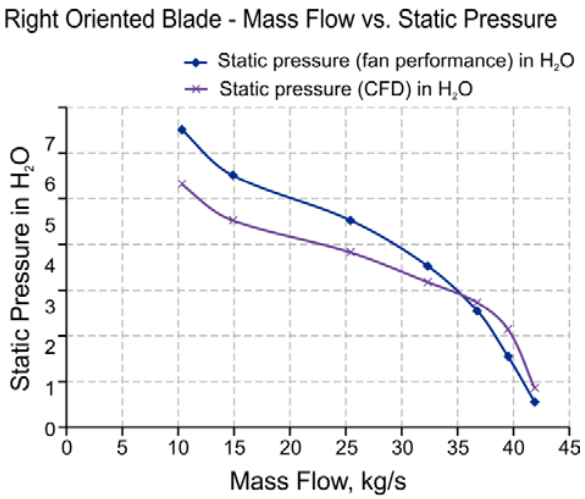

Fig. 15 Experimental vs. CFD performance

IV. Conclusion

The results from the numerical simulations provided an insightful understanding of the behavior of fluid flow around the different fan blade orientations. Numerical CFD analysis was performed for a fan with a left and right oriented blade. The numerical CFD results were then compared with the experimental data. The key and important outcomes of this study are as follows:

1. The CFD modeling shown in this study proved to be very helpful in initiating further and more comprehensive numerical study of the off-road engine cooling system.
2. CFD results were presented in the form of velocity vectors and path lines, which provided actual flow characteristics of air around the fan for different blade orientations.
3. Detection of high and low air flow regions with re-circulations and vortices immensely improved understanding of flow in the complex system studied, which helped to understand the complications involved in hot air recirculation.
4. This study showed how the flow of air was interrupted by the hub obstruction, thereby resulting in unwanted reverse flow regions.
5. The different orientation of blades was also considered while performing CFD analysis. The study revealed that a left oriented blade fan with counterclockwise rotation performed the same as a right oriented blade fan with clockwise rotation.
6. The CFD results were in agreement with the experimental data measured during physical testing. Any error was probably a result of the experimental conditions, fluctuations of fan rev/min, or the considered ideal condition while simulating the analysis.

Acknowledgment

The authors thank the management of Halliburton for their support and permission to publish this paper. They also express gratitude to all of the team members who contributed to the job design, preparation, and execution of the operation to achieve the results presented in this paper.

References

[1] K. Duvenhage, J. A. Vermeulen, C. J. Meyer, and D. G. Kroger, "Flow Distortions at the Fan Inlet of Forced-Draught Air-Cooled Heat Exchanger," in Applied Thermal Engineering, Vol. 16, Nos. 8/9, pp. 741–752, 1996.

[2] F. W. Yu and K.T. Chan, "Modelling of a Condenser-Fan Control for an Air-Cooled Centrifugal Chiller," in Applied Energy Vol. 84, pp. 1117–1135, 2007.

[3] E. H. Twizell and N. J. Bright, "Numerical Modelling of Fan Performance," in Applied Mathematical Modelling, Vol. 5, 1981.

[4] J. R. Bredell, D. G. Kroger, and G. D. Thiart, "Numerical Investigation of Fan Performance in a Forced Draft Air-Cooled Steam Condenser," in Applied Thermal Engineering, Vol. 26, pp. 846–852, 2005.

[5] J. Stafford, E. Walsh, V. Egan, and R. Grimes, "Flat Plate Heat Transfer With Impinging Axial Fan Flows," in International Journal of Heat and Mass Transfer, Vol. 53, pp. 5629–5638, 2010.

[6] J. Stafford, E. Walsh, and V. Egan, "Local Heat Transfer Performance and Exit Flow Characteristics of a Miniature Axial Fan," in International Journal of Heat and Fluid Flow, Vol. 31, pp. 952–960, 2010.

[7] S. H. Ho, L. Rosario, and M. M. Rahman, "Thermal Comfort Enhancement by Using a Ceiling Fan," in Applied Thermal Engineering, Vol. 29, pp. 1648–1656, 2009.